

THE RHIC E-LENS TEST BENCH EXPERIMENTAL RESULTS *

X. Gu[#], F.Z. Altinbas, J. Aronson, E. Beebe, W. Fischer, D.M. Gassner, K. Hamdi, J. Hock, L. Hoff, P. Kankiya, R. Lambiase, Y. Luo, M. Mapes, J. Mi, T. Miller, C. Montag, S. Nemesure, M. Okamura, R. H. Olsen, A.I. Pikin, D. Raparia, P. J. Rosas, J. Sandberg, Y. Tan, C. Theisen, P. Thieberger, J. Tuozzolo, and W. Zhang, BNL, Upton, NY 11973

Abstract

To commission some of the hardware and software for the RHIC electron lenses (e-lenses), we built a test bench based on BNL's EBIS test stand. Over several months, we tested the electron gun, the collector, the high-voltage gun-modulator, the instrumentation, the partial control system, and several software applications. A nominal DC-beam current of 0.85 A was demonstrated. And the electron beam transverse profiles were verified as being Gaussian with a small flat top. We also evaluated some e-lens power-supplies and the electronics for measuring current on our bench. The properties of the cathode and the profile of the beam were assessed. In this paper, we present some of our experimental findings.

INTRODUCTION

To improve the luminosity of the polarized protons in the Relativistic Heavy Ion Collider (RHIC), we are installing two electron lenses (e-lenses) in IR10 [1-4] to compensate for the head-on beam-beam effect. We designed an e-lens test bench to test some elements of the e-lens hardware, its controls, and some application software [5]. Figure 1 illustrates the layout of e-lens test bench; it encompasses an electron source, a beam-propagation system, an electron collector, and some instruments for beam diagnostics.

The electron source is an electron gun with a cathode designed to generate a beam with transverse Gaussian profile [3, 6]. After manufacturing it, we measured the actual shape of the cathode (its cross-sectional profile),

then simulated the beam profile resulting from the cathode profile with the 2D program TRAK, and compared it to the obtained beam profile with the measured beam.

The system that propagates the beam encompasses a 4.6 T superconducting solenoid, a collector coil, gun dipoles, main dipoles, collector dipoles, and a drift tube.

When the electron beam arrives at the collector, we measured its current with the DCCT and the pulse CT [7]. The maximum temperature on the collector was determined by Resistance Temperature Detectors (RTDs) at the highest DC load. The eight RTDs on the cylindrical surface of the electron collector were arranged in two groups. Each group consisted of four RTDs in one longitudinal plane; the four thermocouples of one group were separated azimuthally by 90 degrees, while the two groups were separated longitudinally by 70 mm.

After several months of operation, we tested the electron gun, the collector, the high-voltage gun modulator and most of the instrumentation on the test bench. We also qualified parts of the control system and several software applications. The nominal pulse and the DC beam current of 0.85 A were demonstrated, and the electron beam transverse profiles were verified as being Gaussian. Some e-lens power supplies and the electronics for measuring the current were also assessed. The properties of the cathode and the profile of the beam were evaluated.

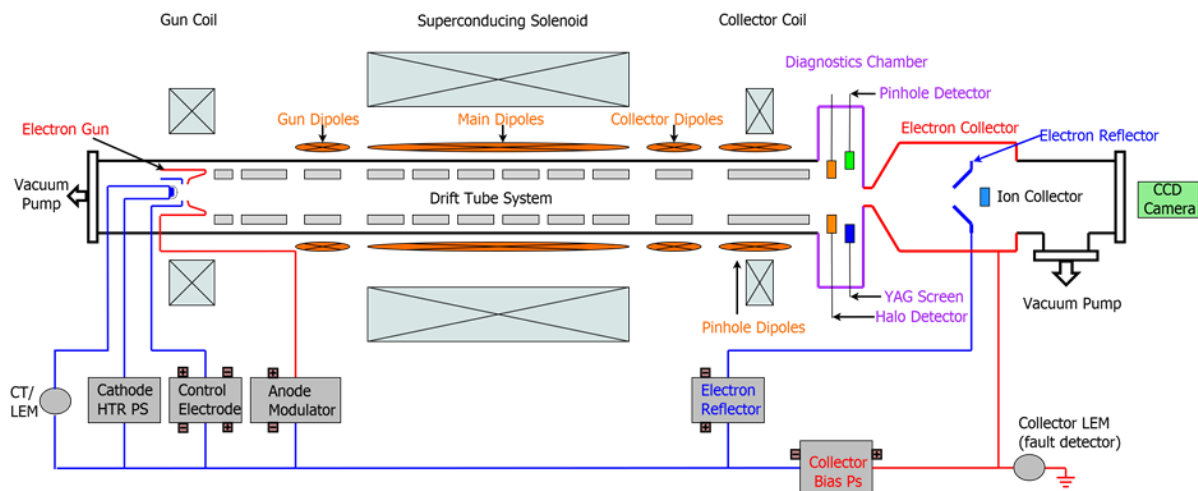


Figure 1: Layout of the electron lens test bench.

* Work supported by Brookhaven Science Associates, LLC under Contract No. DE-AC02-98CH10886 with the U.S. Department of Energy

[#]xgu@bnl.gov

THE ELECTRON GUN AND BEAM

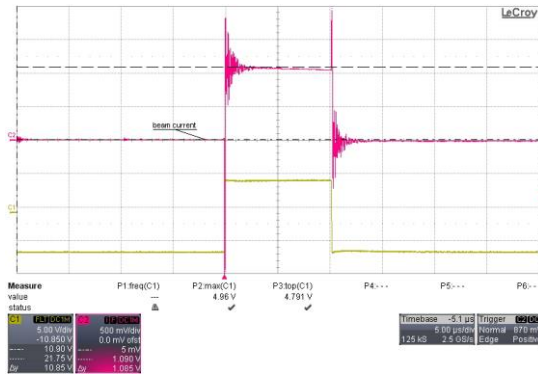


Figure 2: Example of the measurements of the 1085 mA current of the electron beam (yellow) and the anode voltage (red).

We demonstrated the capability of the electron gun on the test bench. Figure 2 shows an example of the measurements of the electron beam current (yellow) and the anode voltage (red). For the current, it is 500 mA/div; for the anode voltage, it is 5 kV/div; the pulse length is 5 μs/div.

For the pulsed electron-beam, we used the gun-side pulse CT (Fig. 1) and obtained the anode voltage locally via the Tek P6015A probe. To obtain information on the beam loss, we evaluated the electron beam current on the collector side CT, and compared it with a similar measurement from the gun-side CT.

THE COLLECTOR

The temperature of the collector was recorded while the DC beam current was being increased to 1 A.

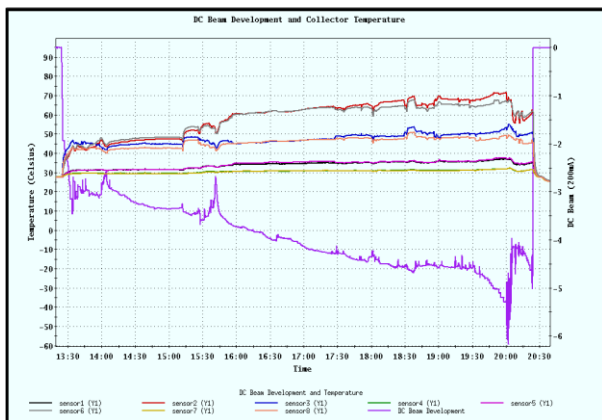


Figure 3: Collector temperature and DC beam.

Figure 3 shows the DC beam current (purple) and the RTDs temperature read-backs (other colors). The DC current is $I = 5.04 \times 200 \text{ mA} = 1080 \text{ mA}$, and the collector voltage is about 5 kV. The total beam power is 5.4 kW and the maximum temperature is about 70°C on the temperature sensor 2.

As it is apparent from Fig. 3, the eight temperature sensors yield four similar groups of readings, implying that the electron beam may be off-axis or not parallel to

the collector axis. Similar readings were obtained from pairs of sensors located at the same angle along the beam, but at two different longitudinal positions.

THE MODULATOR

Figure 4 shows results from the modulator running at 80 kHz with a 10 kV anode voltage. The yellow waveform is the anode voltage, while the red waveform represents the electron beam current measured by the gun-side of the pulse current transformer. The two spikes on both sides of each pulse seemingly reflect the charging and discharging current between the modulator and the anode.

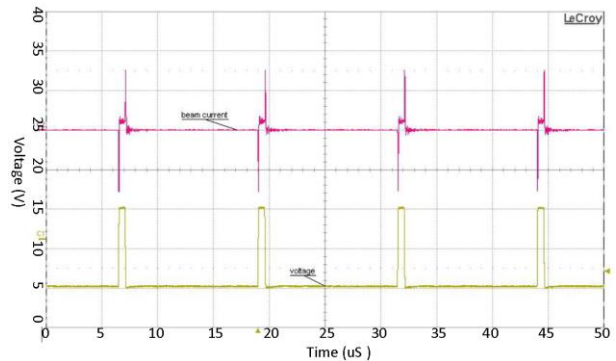


Figure 4: 80 kHz modulator test with beam-current pulse (red), and the anode-voltage pulse (yellow).

The BPMs will play a critical role in meeting the ambitious requirements for commissioning and operating the electron lenses. Two BPMs in the e-lens will measure the positions of both the proton and the electron beam. To assure beam alignment within 10% beam sigma precision for a 300-μm electron beam, we designed the modulator with a rise and fall time of only 50 ns.

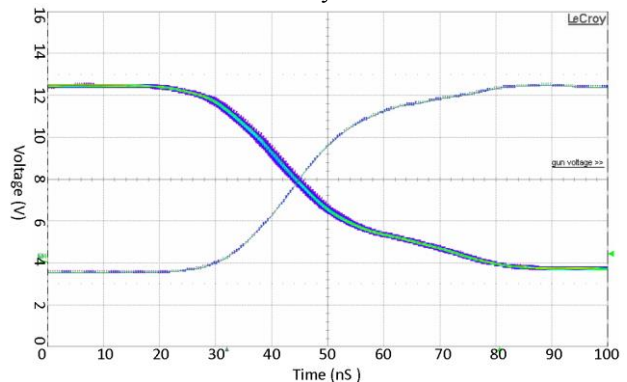


Figure 5: Rise and fall times of the electron beam measured via the anode voltage.

Although the beam current is a non-linear function of the voltage, the rise and fall times of the current signal are very close to the rise and fall times of the anode's voltage signal. Therefore, at first, we measured the electron beam rise and fall times via measuring those of the anode voltage.

Figure 5 plots the beam rise and fall time, measured with a waveform persistence setup; it reveals that the

rising edge of the beam is more stable than the falling edge. The frequency is 80 kHz, and the anode voltage is 10 kV.

The rise and fall times for 98% of the amplitude are 60 ns and 70 ns, respectively. We located the Behlke switch of the anode modulator about 0.6 m away from the anode because of the test bench structural limitations. We will reduce the contribution of the capacitance and inductance of the connecting cable to the transitions of the modulator pulses in the e-lens by positioning the Behlke switch much closer, i.e., 10 cm, to the anode feed-through.

PINHOLE SCANNER AND YAG SCREEN

The pinhole scanner was fully tested, evaluated, and calibrated. By adding a bias voltage on the pinhole we found that the behaviour of the secondary electrons play an important role in the total signal at the integral pinhole scanner.

Figure 6 shows the beam profile, acquired by the pinhole scanner for a beam of 200 mA. The profile has a flat top at the center, and lesser intensity at the edges of the beam, as predicted by the 2D program TRAK with a measured cathode profile.

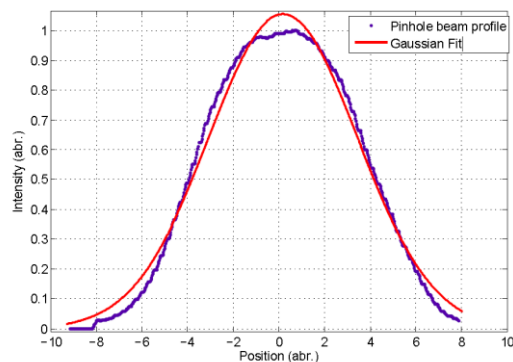


Figure 6: Beam profile obtained using pinhole scanner.

We also developed a YAG screen and camera system for measuring the beam profile. Our findings for a 144 mA electron beam are plotted in Fig. 7; the profile is similar to that depicting the pinhole results.

The YAG screen can obtain the beam profile within seconds. We acquired many beam profiles for different system configurations. However, caution is required here because the YAG screen is very fragile and can be damaged by unwanted beam current.

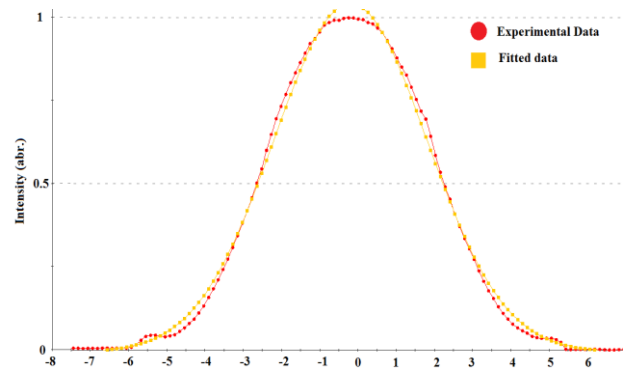


Figure 7: Beam profile from YAG screen, showing the correspondence between the experimental and fitted data.

SUMMARY

We tested and improved the electron gun, collector, some instrumentation, and some power supplies on the e-lens test bench. The software- and the machine-protection system were also prototyped. All of these tests resulted in a considerable savings in time for commissioning the 2013 e-lens, and later on.

ACKNOWLEDGMENTS

The authors would like to acknowledge the help of the instrumentation, vacuum and controls groups. The authors are also grateful for the valuable discussions with the FNAL TEL staff, in particular with V. Shiltsev, A. Valishev, and G. Stancari.

REFERENCES

- [1] W. Fischer, et al., "Status of head-on beam-beam compensation in RHIC", proceedings of the ICFA Mini-Workshop on Beam-Beam Effects in Hadron Colliders (BB3013), CERN (2013).
- [2] X. Gu, et al., "Designing a Beam Transport System for RHIC's Electron Lens", PAC'11, New York, USA TUP208.
- [3] A. Pikin, et al., "Structure and Design of the Electron Lens for RHIC", PAC'11, New York, USA THP100.
- [4] X. Gu, et al., "The Effects of The RHIC e-lenses Magnetic Structure Layout on The Proton Beam Trajectory", PAC'11, New York, USA TUP207.
- [5] J.G. Alessi, et al., "Progress on Test EBIS and the Design of an EBIS-based RHIC Preinjector", PAC'05, Knoxville, Tennessee, P363.
- [6] Y. Luo, et al., "6-D weak-strong simulation of head-on beam-beam compensation in the Relativistic Heavy Ion Collider". Phys. Rev. ST Accel. Beams 15, 051004 (2012).
- [7] D. M. Gassner, et al., "RHIC Electron Lens Test Bench Diagnostics". DIPAC'11, Hamburg, Germany, MOPD04.